

Rostral and dorsal anterior cingulate cortex make dissociable contributions during antisaccade error commission

Frida E. Polli^{†‡§}, Jason J. S. Barton[¶], Matthew S. Cain[†], Katharine N. Thakkar[†], Scott L. Rauch[†], and Dara S. Manoach^{†||}

[†]Department of Psychiatry, Massachusetts General Hospital, Harvard Medical School, Boston, MA 02215; [‡]Department of Psychology, Suffolk University, Boston, MA 02114; [¶]Departments of Neurology, Ophthalmology, and Visual Sciences, University of British Columbia, Vancouver, BC, Canada V6T 1Z4; and ^{||}Athinoula A. Martinos Center for Biomedical Imaging, Charlestown, MA 02129

Edited by Edward E. Smith, Columbia University, New York, NY, and approved September 8, 2005 (received for review May 5, 2005)

The anterior cingulate cortex (ACC) participates in both performance optimization and evaluation, with dissociable contributions from dorsal (dACC) and rostral (rACC) regions. Deactivation in rACC and other default-mode regions is important for performance optimization, whereas increased rACC and dACC activation contributes to performance evaluation. Errors activate both rACC and dACC. We propose that this activation reflects differential error-related involvement of rACC and dACC during both performance optimization and evaluation, and that these two processes can be distinguished by the timing of their occurrence within a trial. We compared correct and error antisaccade trials. We expected errors to correlate with an early failure of rACC deactivation and increased activation of both rACC and dACC later in the trial. Eighteen healthy subjects performed a series of prosaccade and antisaccade trials during event-related functional MRI. We estimated the hemodynamic responses for error and correct antisaccades using a finite impulse-response model. We examined ACC activity by comparing error and correct antisaccades with a fixation baseline and error to correct antisaccades directly. Compared with correct antisaccades, errors were characterized by an early bilateral failure of deactivation of rACC and other default-mode regions. This difference was significant in rACC. Errors also were associated with increased activity in both rACC and dACC later in the trial. These results show that accurate performance involves deactivation of the rACC and other default mode regions and suggest that both rACC and dACC contribute to the evaluation of error responses.

default-mode network | performance evaluation | task-induced deactivation | inhibition | cognition

Electrophysiological and neuroimaging studies consistently report anterior cingulate cortex (ACC) activity during error commission (1–5). The ACC, however, is a heterogeneous structure that can be parsed into dorsal (dACC) and rostral (rACC) regions based on cytoarchitecture, function, and connectivity (6–9). The dACC extends caudally from the genu of the corpus callosum to the vertical plane of the anterior commissure and connects with the lateral prefrontal cortex and hippocampus to regulate effortful cognitive operations. The rACC lies anterior and ventral to the genu of the corpus callosum and forms a circuit with the amygdala, insula, and ventral striatum to oversee emotional processing (for review, see ref. 10). Given these specializations, it is likely that the dACC and rACC make different contributions during error commission. In the present study, we examined activity in both these regions during different phases of error commission.

Error-related activity in both rACC and dACC is thought to reflect their contributions to performance evaluation (2, 5, 11). The dACC is believed to be the primary generator of the error-related negativity (ERN) (5, 12), an event-related potential occurring 80–180 ms post-error (13), although a generator in the medial prefrontal cortex (PFC) has also been reported (14). Two chief theories exist regarding the functional significance of the ERN and

dACC activity: error detection (13, 15) and conflict monitoring (4) (for review, see ref. 16). Both theories posit that the dACC interacts with the lateral PFC to effect changes in future response selection based on feedback from previous responses. Error-related rACC activity is less consistently observed with functional MRI (2, 3, 11) than dACC activity (1), and the role of rACC in error processing is less well understood. The rACC also has been implicated in ERN generation (14), consistent with the finding that ERN amplitude correlates with negative affect (17, 18). The error positivity, an event-related potential occurring 300–500 ms post-error, has also been localized to the rACC (5). Error-positivity amplitude correlates with error awareness (19), skin-conductance response during error commission (20), and negative affect (17). These findings suggest that the rACC is involved in the affective appraisal of errors.

In addition to their role in performance evaluation, rACC and dACC are thought to play reciprocal roles in performance optimization (21). With demanding cognitive activity, dACC activity increases while rACC activity decreases [i.e., task-induced deactivation (TID)] (9, 21, 22). In addition to the rACC, TID also is observed in regions comprising the default-mode network, including the orbitofrontal cortex, posterior cingulate cortex, superior temporal cortex, dorsomedial PFC, and angular gyrus (22–25). The putative function of TID in rACC and other default-mode regions is to optimize performance by allocating resources to task-necessary regions and away from task-extraneous ones (21). This hypothesis is consistent with findings that performance impairments correlate with increased activity in rACC and other default-mode regions (26). Thus, increased error-related rACC activity might reflect its contribution to both performance optimization and evaluation. These two processes could be distinguished by the timing of their occurrence within a trial: activity related to performance optimization should precede activity related to performance evaluation. While dACC and presupplementary motor area activity is known to increase during response preparation and to decrease prior to an error (27, 28), the timing and relationship of TID in rACC and associated regions to error vs. correct responding have not been determined.

In the present study, we used a saccadic task and rapid-presentation, event-related functional MRI to examine dACC and rACC activity during error commission. Event-related functional MRI allows us to determine whether TID fails specifically during error trials, and the timing of its occurrence within a trial. The task consists of a pseudorandom sequence of prosaccade (PS) and antisaccade (AS) trials. PS trials require the simple prepotent

This paper was submitted directly (Track II) to the PNAS office.

Freely available online through the PNAS open access option.

Abbreviations: AS, antisaccade; PS, prosaccade; ACC, anterior cingulate cortex; dACC, dorsal ACC; rACC, rostral ACC; TID, task-induced deactivation; ERN, error-related negativity; PFC, prefrontal cortex; HDR, hemodynamic response.

[§]To whom correspondence should be addressed at: CNY 149, Room 2608, 13th Street, Charlestown, MA 02129. E-mail: fpolli@nmr.mgh.harvard.edu.

© 2005 by The National Academy of Sciences of the USA

response of looking toward a suddenly appearing visual target. AS trials require the suppression of the prepotent PS and the substitution of the novel behavior of looking in the opposite direction. We restricted our comparisons of correct and error responses to ASs because errors occur almost exclusively on AS trials in healthy subjects on this task (29). Moreover, AS performance has been associated with TID in rACC and other default-mode regions (30), and AS errors generate robust performance evaluation indices (e.g., ERN and error positivity) (19). We hypothesized that, compared with correct ASs, AS errors would be characterized by (i) decreased TID in rACC and other default-mode regions early in the trial, reflecting a failure of performance optimization, and (ii) increased activity in both rACC and dACC later in error trials, consistent with their purported roles in performance evaluation. We also investigated whether early rACC activity would correlate with error rate in individual subjects, consistent with the notion that a failure of TID would compromise performance. Finally, because TID in rACC (and other default-mode regions) during ASs may arise from activation of these regions during fixation (31), we also compared correct ASs with correct PSs to determine whether there was differential TID.

Methods

Subjects. Twenty-one subjects were recruited from the community by poster and web-site advertisements. Data from three subjects were excluded, two because of eye-tracker malfunction and one because of near-perfect (0.5% error rate) AS performance. Analyses were conducted on the remaining 18 subjects (11 male, 7 female; mean age, 33 ± 11 years). All subjects were strongly right-handed (mean Edinburgh score, 90 ± 12) (32). Before scanning, subjects practiced the task. Subjects were instructed to respond as quickly and accurately as possible and were told that they would receive a five-cent bonus for each correct response, an incentive intended to mitigate fatigue and boredom.

Apparatus. Images were acquired with a 3.0-T Trio whole-body high-speed imaging device equipped for echoplanar imaging (EPI) (Siemens, Iselin, NJ). Head stabilization was achieved with cushioning, and all subjects wore earplugs to attenuate noise. Eye-movement stimuli were generated by a Macintosh G4 Power Mac using programs written in C++ on the VISION SHELL programming platform (MicroML, St. Hyacinthe, Quebec) and back-projected with a color liquid-crystal display projector (Sharp, XG-2000, Osaka, Japan) onto a screen positioned on the head coil. The ISCAN functional MRI Remote Eye-Tracking Laboratory (Burlington, MA) recorded saccades during scanning. This system used a video camera mounted at the rear of the MRI bore. The camera imaged the eye of the prone subject through an optical combiner, a 45° cold transmissive mirror that reflects an infrared image of the eye. Infrared illumination was provided by a small light-emitting diode cluster mounted on the head coil. Eye images were processed by ISCAN's RK-726PCI high-resolution pupil/corneal reflection tracker. Eye position was sampled at 60 Hz.

Saccadic Paradigm. Each saccadic trial lasted 4,000 ms (Fig. 1). Trials began with a 300-ms instructional cue at screen center. For half of the subjects, a yellow ring and blue cross were the cues for PS and AS trials, respectively. The cues were reversed for the remaining subjects. The cue was flanked horizontally by two small white dots of 0.2° diameter that marked the potential locations of targets, 10° left and right of center. These dots remained on the screen for the duration of each run. The cue was then replaced by a white fixation ring at the center with a diameter of 0.4° and a luminance of 20 cd/m². After 1,700 ms, the ring shifted to one of the two target locations chosen at random. This ring was the target to which the subject responded. The ring remained in the peripheral location for 1,000 ms, then returned to the center, where subjects were required to return their gaze for 1,000 ms before the start of the next trial.

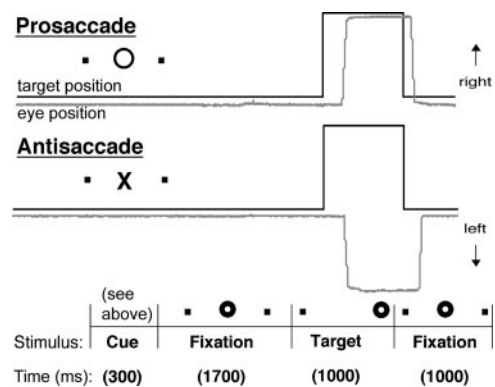


Fig. 1. Schematic depiction of a 4,000-ms saccadic trial. Trials began with a 300-ms cue instructing participants to make either a PS or an AS. The cue was then replaced by a fixation ring, which shifted to one of two target locations flanking the cue horizontally. This target was the one to which subjects responded. The ring remained in the peripheral location for 1,000 ms, then returned to the center for 1,000 ms.

Randomly interleaved with the saccadic trials were 2-, 4-, or 6-s fixation trials. Subjects performed six runs of the task, with short rests between runs. Each run consisted of a random sequence of PS (26–46), AS (24–46), and fixation trials (10–17), and lasted 5 min 22 s each. A technique to optimize the statistical efficiency of event-related designs determined the schedule of events (33). The total experiment lasted ≈ 45 min and generated a total of 200 PS and 200 AS trials and 79 fixation trials.

Image Acquisition. Automated shimming procedures were performed, and scout images were obtained. Two high-resolution structural images were acquired for spatial normalization and cortical surface reconstruction using a 3D MPRAGE sequence [repeat time (TR)/echo time (TE)/Flip = 2530 ms/3 ms/7°; voxel size, $1.3 \times 1.3 \times 1$ mm], T1- and T2-weighted structural images with the same slice specifications as the blood oxygenation level-dependent (BOLD) scans were obtained to assist in registering functional and structural images. Functional images were collected using a gradient echo T2*-weighted sequence (TR/TE/Flip = 2,000 ms/30 ms/90°). Twenty contiguous horizontal slices parallel to the intercommissural plane (voxel size, $3.13 \times 3.13 \times 5$ mm) were acquired interleaved. The functional sequences included prospective acquisition correction (PACE) for head motion (34). PACE adjusts slice position and orientation in real time during data acquisition, which reduces motion-induced effects on magnetization history.

Analysis of Imaging Data. All analyses were done by using FREESURFER (35) and FREESURFER FUNCTIONAL ANALYSIS STREAM (FS-FAST) (36) software. In addition to online motion correction (PACE), functional scans were corrected retrospectively for motion using the AFNI algorithm (37), intensity-normalized, and smoothed using a 3D 8-mm full width at half maximum (FWHM) Gaussian kernel. Functional scans were aligned to the averaged MPRAGE structural scans. The averaged MPRAGE scans were also used to construct inflated (2D) models of individual cortical surfaces using an automated procedure involving segmentation of gray and white matter (38), tessellation of the gray/white border (35), and inflation of the folded cortical surface (39). Each subject's reconstructed brain was then transformed using sulcal/gyral patterns to an average spherical surface representation (35). This representation provided a 2D surface-based spherical coordinate system onto which functional data were resampled after further smoothing with a 2D 8-mm FWHM Gaussian kernel (40). Cortical activity was localized using an automated surface-based parcellation system

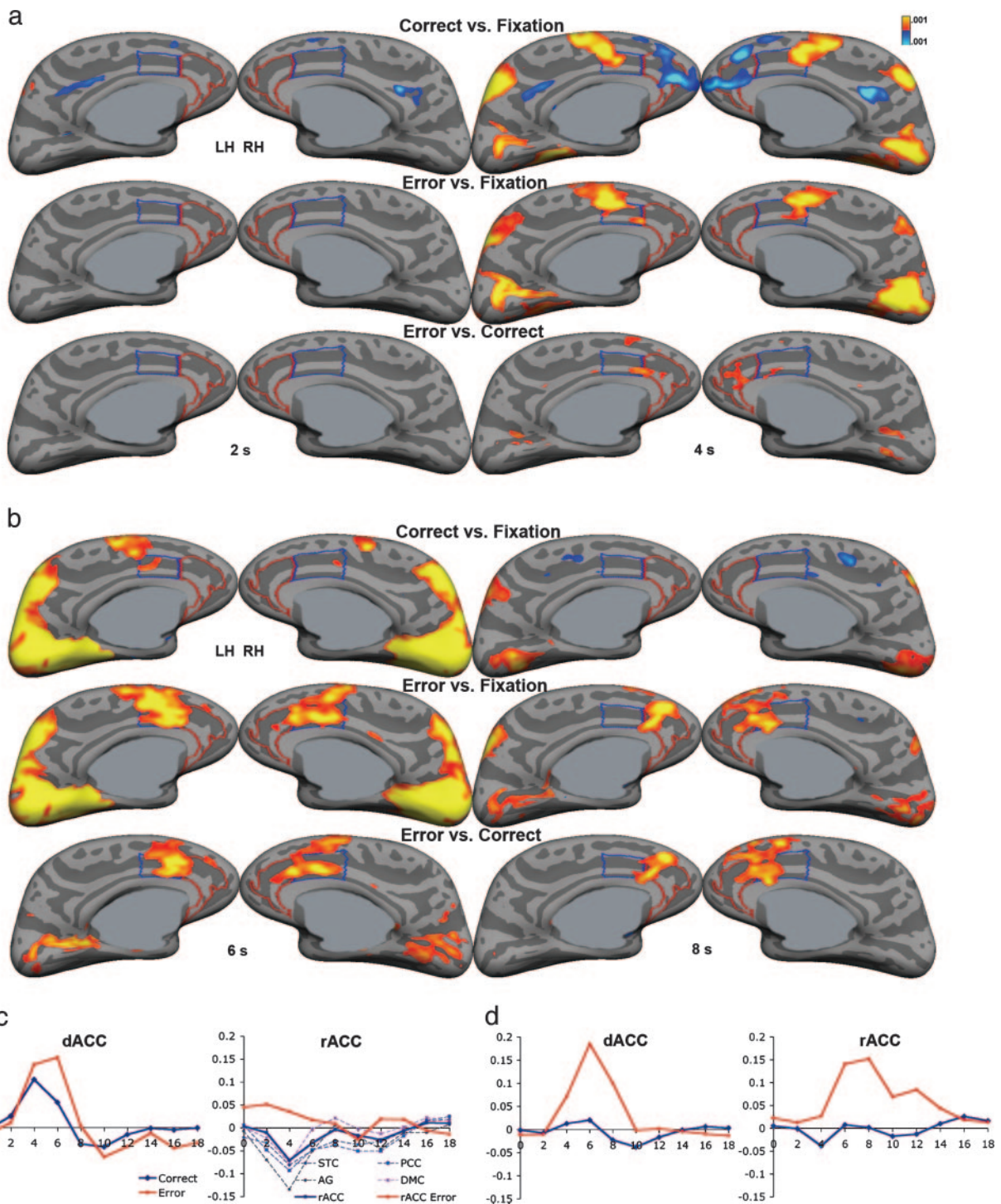


Fig. 2. Findings of differential rACC and dACC activity at early and later time points during correct and error antisaccade trials. Statistical activity maps displayed on the inflated medial cortical surfaces for the three contrasts (correct ASs vs. fixation, error ASs vs. fixation, and error vs. correct ASs) for the two early time points, 2 and 4 s (**a**), and the two later time points, 6 and 8 s (**b**). Gray masks cover noncortical regions in which any activation is displaced. (**c**) The HDRs for the dACC and rACC, as well as posterior cingulate cortex (PCC), dorsomedial PFC (DMC), superior temporal cortex (STC), and angular gyrus (AG) minima in the correct vs. fixation contrast. (**d**) The HDRs for the dACC and rACC maxima in the error vs. correct contrast. Time in seconds is on the x axis, and percent signal change relative to the fixation baseline is on the y axis. All HDRs are an average of left- and right-hemisphere minima/maxima HDRs. Although clusters $<120 \text{ mm}^2$ are displayed, they are not considered significant.

(41). The ACC was divided into dorsal and rostral regions using a line drawn at the anterior boundary of the genu of the corpus callosum that was perpendicular to the intercommisural plane (6).

A finite impulse-response model (36) was used to estimate the event-related hemodynamic responses (HDRs) for each of the four

trial types (correct PSs, error PSs, correct ASs, and error ASs) for each subject. A finite impulse-response model uses a linear model to provide unbiased estimates of the average signal intensity at each time point for each trial type, rather than making *a priori* assumptions about the shape of the HDR. We used 12 time points with an

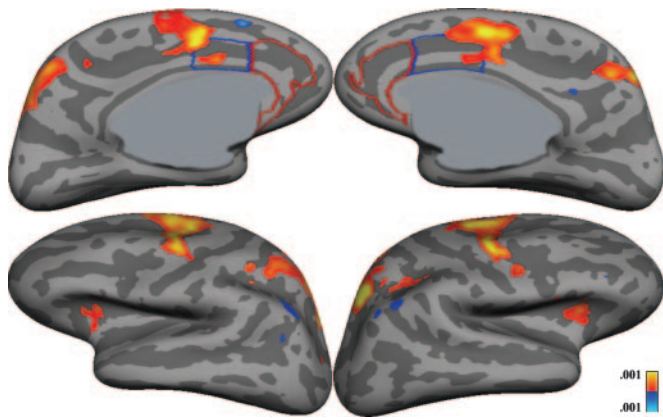


Fig. 4. Statistical maps displayed on the inflated medial and lateral cortical surfaces for the correct AS vs. PS trials at 4 s.

maxima, 10.0, 2.8, 32.5; cluster size, 187 mm²) (Fig. 3), where increased activity correlated with a lower error rate.

Discussion

Consistent with our hypotheses, rACC and dACC were differentially involved in the early and late phases of error commission. In the early phase of the trial, correct, but not erroneous, AS performance was associated with bilateral deactivation of the rACC and other regions thought to comprise the default-mode network. This result suggests that deactivation of rACC and associated default-mode regions is associated with accurate task performance. In contrast, dACC and neighboring supplementary motor area and presupplementary motor area showed increased activity early in both error and correct trials and did not differ between them. This finding, along with the finding that early increased activity in dACC was associated with fewer errors, suggests that these regions contribute to effortful cognitive performance and/or conflict monitoring. In the later phase of the trial, relative to correct trials, AS errors were associated with increased activity in both rACC and dACC. This result is consistent with previous findings that implicate these regions in performance evaluation (1). More generally, our findings suggest that rACC and dACC make distinct contributions to the optimization and evaluation of cognitive performance over the course of a trial.

These findings are consistent with other evidence that TID in task-extraneous regions facilitates optimal performance, and that its absence is associated with performance decrements (26, 47). These findings extend this work in two important ways. First, they demonstrate that TID occurs during correct but not error trials. This association may have been missed by previous studies of error commission that compared error trials with correct trials but not to a baseline condition. A baseline comparison is necessary to resolve whether differential activity between two conditions, such as error vs. correct trials, is due to a relative increase in activation during errors, a relative decrease in activation during correct trials, or both (24). Two studies that compared error and correct trials with fixation did not report differential TID between the two conditions (2, 47). Differences in various factors that influence TID, including stimulus presentation rate and task difficulty (48), may account for discrepant findings.

The second extension of previous work concerns the timing of TID. Using an event-related design, we found that TID in the default-mode network during correct trials began 2 s after cue presentation, was significantly different from baseline at this time point in superior temporal cortex and posterior cingulate cortex, and was maximal throughout the network at the 4-s time point. Increased dACC/presupplementary motor area activity followed the same pattern. Activity in rACC and dACC during error trials,

presumably related to performance evaluation, showed a different pattern of activity. It began 2 s after target presentation at the 4-s time point and peaked at the 6- and 8-s time points. These results demonstrate that TID during correct trials occurs earlier than increased rACC/dACC activity during error trials. We interpret this finding to reflect that TID is preparatory whereas increased ACC activity is evaluative.

However, our interpretations regarding the exact roles of TID vs. increased ACC activity must be tempered, given the limited temporal resolution provided by the paradigm that we used. Although a longer cue-target delay might have provided greater temporal sensitivity, TID increases with faster stimulus presentation rate (48), and, therefore, we believed that a short cue-target delay would maximize TID. A variable cue-target delay would have allowed us to model the cue and target separately, but this temporal jitter would not have been possible in the context of a finite impulse-response design while maintaining a short cue-target delay. Thus, the fixed timing and short duration (2 s) of the delay prevented us from unequivocally distinguishing cue from response-related hemodynamic activity. Therefore, given event-related potential studies showing that the ERN occurs almost immediately after post-error (13), peak hemodynamic activity at the 4-s time period, instead of reflecting performance optimization activity, may reflect response-related activity. If the hemodynamic activity at 4 s were related to the response, it would indicate that TID was occurring during or after response execution, rather than before. However, the regions that show a peak response at 6 s have been consistently implicated in performance evaluation (1), whereas the regions that peak at 4 s are more consistently implicated in performance optimization (28, 47). Thus, the hypothesis that peak TID at 4 s reflects activity related to the response would suggest that there were two distinct phases of evaluative activity. The hypothesis that peak TID at 4 s is related to performance optimization is more consistent with previous work and provides a more parsimonious explanation of our findings. Nonetheless, although this study has established differential TID during error vs. correct responding and suggested timing differences between TID and evaluation activity, future studies are needed to more precisely delineate the timing of the two processes.

The finding of increased dACC and rACC activity later in error vs. correct trials is consistent with previous error studies (1) and supports the hypothesis that these regions are involved in the evaluation of the error response. Examination of the HDRs demonstrates differential timing of the dACC and rACC responses to errors that are consistent with their proposed cognitive and affective specializations. It is possible that the fast rise and sharp fall of activity in dACC reflect a role in updating of stimulus-response mappings immediately after the error response (49), whereas the more gradual rise, later peak, and slower fall of rACC activity could be consistent with a role in the affective appraisal of the error (20). The reward for correct responses represents a potential confound in the interpretation of increased error-related activity in the dACC, given the demonstrated sensitivity of this region to reward loss (50). Reward loss has not been associated with changes in TID, however, and is, therefore, unlikely to account for the finding of TID failure with errors.

The current findings also enhance our understanding of ACC function by showing that rACC and dACC have reciprocal activation patterns during correct performance yet similar activation patterns during erroneous performance. Interestingly, different regions of the rACC and dACC, both of which are comprised of several Brodmann areas, appeared to be maximally involved in performance optimization vs. evaluation. Consistent with other studies, performance optimization activity appeared maximal in the sulcus of the rACC (24–26) and in posterior dACC bordering on presupplementary motor area (27), whereas later performance evaluation activity was maximal on the gyrus of rACC (2, 3, 11) and

in anterior dACC (1). However, these finer anatomical distinctions may strain the limits of spatial resolution.

Finally, it is possible that deactivation in the default-mode network during AS performance resulted from increased activation of these regions during fixation (31). To address this issue, we contrasted correct ASs with the nonfixation baseline of correct PSs and found significant TID differences only in the left angular gyrus. These results differ from those of a previous block-design study that reported increased TID in ventromedial PFC with ASs vs. PSs (30). These differences may arise from the current paradigm presenting trials in a pseudorandom order rather than in single-trial blocks. This design gives rise to increased working memory requirements and task-switching costs (29). In this context, PSs may have been more cognitively demanding than the block PSs of previous studies. Because TID increases with task difficulty (48), more difficult PSs would lead to less differential TID between ASs and PSs. The use of PSs as a nonfixation baseline also does not address the central question of whether TID during correct ASs vs. fixation represents deactivation during AS trials or activation during fixation. A positron-emission tomography study assessing an absolute measure of brain activity, namely oxygen extraction fraction, reported that

oxygen extraction fraction in rACC and other default-mode regions did not differ significantly from its mean throughout the brain during fixation (24). This finding suggests that differences of the magnitude observed in rACC between correct ASs vs. fixation are unlikely to be accounted for by increased rACC activity during fixation.

The finding of TID failure during errors provides a possible mechanism for emotional interference of cognition by emotion. Negative emotional states are known to increase rACC activity (21) and impair performance accuracy (51) in healthy controls. TID failure also may contribute to cognitive dysfunction in depression and obsessive compulsive disorder, both of which are associated with increased rACC metabolism (52, 53) and impaired cognitive performance (54). A better delineation of the systems responsible for the dynamic optimization and evaluation of cognitive performance may elucidate the basis of performance variation in both health and disease.

We thank Dr. George Bush for his thoughtful comments. This work was supported by National Institute of Mental Health Grants F31 MH72120 (to F.E.P.), R01 MH67720 (to D.S.M.), and K08 NS01920 (to J.J.S.B.).

- Hester, R., Fassbender, C. & Garavan, H. (2004) *Cereb. Cortex* **14**, 986–994.
- Kiehl, K. A., Liddle, P. F. & Hopfinger, J. B. (2000) *Psychophysiology* **37**, 216–223.
- Menon, V., Adelman, N. E., White, C. D., Glover, G. H. & Reiss, A. L. (2001) *Hum. Brain Mapp.* **12**, 131–143.
- Carter, C. S., Braver, T. S., Barch, D. M., Botvinick, M. M., Noll, D. & Cohen, J. D. (1998) *Science* **280**, 747–749.
- Van Veen, V. & Carter, C. S. (2002) *J. Cognit. Neurosci.* **14**, 593–602.
- Devinsky, O., Morrell, M. J. & Vogt, B. A. (1995) *Brain* **118**, 279–306.
- Bush, G., Whalen, P. J., Rosen, B. R., Jenike, M. A., McInerney, S. C. & Rauch, S. L. (1998) *Hum. Brain Mapp.* **6**, 270–282.
- Whalen, P. J., Bush, G., McNally, R. J., Wilhelm, S., McInerney, S. C., Jenike, M. A. & Rauch, S. L. (1998) *Biol. Psychiatry* **44**, 1219–1228.
- Bush, G., Luu, P. & Posner, M. I. (2000) *Trends Cognit. Sci.* **4**, 215–222.
- Phillips, M. L., Drevets, W. C., Rauch, S. L. & Lane, R. (2003) *Biol. Psychiatry* **54**, 504–514.
- Garavan, H., Ross, T. J., Kaufman, J. & Stein, E. A. (2003) *NeuroImage* **20**, 1132–1139.
- Dehaene, S., Posner, M. I. & Tucker, D. M. (1994) *Psychol. Sci.* **5**, 303–305.
- Gehring, W. J., Goss, B., Coles, M. G., Meyer, D. E. & Donchin, E. (1993) *Psychol. Sci.* **4**, 385–390.
- Luu, P., Tucker, D. M., Derryberry, D., Reed, M. & Poulsen, C. (2003) *Psychol. Sci.* **14**, 47–53.
- Holroyd, C. B. & Coles, M. G. (2002) *Psychol. Rev.* **109**, 679–709.
- Ullsperger, M. & von Cramon, D. Y. (2004) *Cortex* **40**, 593–604.
- Hajcak, G., McDonald, N. & Simons, R. F. (2004) *Brain Cognit.* **56**, 189–197.
- Luu, P., Collins, P. & Tucker, D. M. (2000) *J. Exp. Psychol. Gen.* **129**, 43–60.
- Nieuwenhuis, S., Ridderinkhof, K. R., Blom, J., Band, G. P. & Kok, A. (2001) *Psychophysiology* **38**, 752–760.
- Hajcak, G., McDonald, N. & Simons, R. F. (2003) *Psychophysiology* **40**, 895–903.
- Drevets, W. C. & Raichle, M. E. (1998) *Cognit. Emot.* **12**, 353–385.
- Binder, J. R., Frost, J. A., Hammeke, T. A., Bellgowan, P. S., Rao, S. M. & Cox, R. W. (1999) *J. Cognit. Neurosci.* **11**, 80–95.
- Shulman, G. I., Fiez, J. A., Corbetta, M., Buckner, R. L., Miezin, F. M., Raichle, M. E. & Petersen, S. E. (1997) *J. Cognit. Neurosci.* **9**, 648–663.
- Raichle, M. E., MacLeod, A. M., Snyder, A. Z., Powers, W. J., Gusnard, D. A. & Shulman, G. L. (2001) *Proc. Natl. Acad. Sci. USA* **98**, 676–682.
- Gusnard, D. A. & Raichle, M. E. (2001) *Nat. Rev. Neurosci.* **2**, 685–694.
- Simpson, J. R., Jr., Snyder, A. Z., Gusnard, D. A. & Raichle, M. E. (2001) *Proc. Natl. Acad. Sci. USA* **98**, 683–687.
- Luks, T. L., Simpson, G. V., Feiwel, R. J. & Miller, W. L. (2002) *NeuroImage* **17**, 792–802.
- Curtis, C. E. & D'Esposito, M. (2003) *J. Cognit. Neurosci.* **15**, 409–418.
- Manoach, D. S., Lindgren, K. A., Cherkasova, M. V., Goff, D. C., Halpern, E. F., Intriligator, J. & Barton, J. J. (2002) *Biol. Psychiatry* **51**, 816–826.
- Sweeney, J. A., Mintun, M. A., Kwee, S., Wiseman, M. B., Brown, D. L., Rosenberg, D. R. & Carl, J. R. (1996) *J. Neurophysiol.* **75**, 454–468.
- Stark, C. E. & Squire, L. R. (2001) *Proc. Natl. Acad. Sci. USA* **98**, 12760–12766.
- Schachter, S. C. (1994) *Int. J. Neurosci.* **77**, 47–51.
- Dale, A. M. (1999) *Hum. Brain Mapp.* **8**, 109–114.
- Thesen, S., Heid, O., Mueller, E. & Schad, L. R. (2000) *Magn. Reson. Med.* **44**, 457–465.
- Fischl, B., Sereno, M. I. & Dale, A. M. (1999) *NeuroImage* **9**, 195–207.
- Burock, M. A. & Dale, A. M. (2000) *Hum. Brain Mapp.* **11**, 249–260.
- Cox, R. W. & Jesmanowicz, A. (1999) *Magn. Reson. Med.* **42**, 1014–1018.
- Dale, A. M. & Sereno, M. I. (1993) *Neuron* **26**, 55–67.
- Fischl, B., Liu, A. & Dale, A. M. (2001) *IEEE Trans. Med. Imaging* **20**, 70–80.
- Sereno, M. I., Dale, A. M., Reppas, J. B., Kwong, K. K., Belliveau, J. W., Brady, T. J., Rosen, B. R. & Tootell, R. B. (1995) *Science* **268**, 889–893.
- Fischl, B., van der Kouwe, A., Destrieux, C., Halgren, E., Segonne, F., Salat, D. H., Busa, E., Seidman, L. J., Goldstein, J., Kennedy, D., et al. (2004) *Cereb. Cortex* **14**, 11–22.
- Forman, S. D., Cohen, J. D., Fitzgerald, M., Eddy, W. F., Mintun, M. A. & Noll, D. C. (1995) *Magn. Reson. Med.* **33**, 636–647.
- Boynton, G. M., Engel, S. A., Glover, G. H. & Heeger, D. J. (1996) *J. Neurosci.* **16**, 4207–4221.
- Dale, A. M. & Buckner, R. L. (1997) *Hum. Brain Mapp.* **5**, 329–340.
- Savoy, R. L. (2001) *Acta. Psychol.* **107**, 9–42.
- Talairach, J. & Tournoux, P. (1988) *Co-planar Stereotaxic Atlas of the Human Brain: 3-Dimensional Proportional System: An Approach to Cerebral Imaging* (Thieme, New York).
- Hester, R. L., Murphy, K., Foxe, J. J., Foxe, D. M., Javitt, D. C. & Garavan, H. (2004) *J. Cognit. Neurosci.* **16**, 776–785.
- McKiernan, K. A., Kaufman, J. N., Kucera-Thompson, J. & Binder, J. R. (2003) *J. Cognit. Neurosci.* **15**, 394–408.
- Ullsperger, M. & von Cramon, D. Y. (2004) *Nat. Neurosci.* **7**, 1173–1174.
- Bush, G., Vogt, B. A., Holmes, J., Dale, A. M., Greve, D., Jenike, M. A. & Rosen, B. R. (2002) *Proc. Natl. Acad. Sci. USA* **99**, 523–528.
- Perlstein, W. M., Elbert, T. & Stenger, V. A. (2002) *Proc. Natl. Acad. Sci. USA* **99**, 1736–1741.
- Drevets, W. C. (2000) *Biol. Psychiatry* **48**, 813–829.
- Rauch, S. L., Jenike, M. A., Alpert, N. M., Baer, L., Breiter, H. C., Savage, C. R. & Fischman, A. J. (1994) *Arch. Gen. Psychiatry* **51**, 62–70.
- Zakzanis, K. K., Leach, L. & Kaplan, E. (1999) *Neuropsychological Differential Diagnosis* (Swets & Zeitlinger, Lisse, The Netherlands).